Thermal Stability of the DNA-Binding Domain of the Myb Oncoprotein†

A. Sarai,*,‡ H. Uedaira,§ H. Morii,§ T. Yasukawa,‡,∥ K. Ogata,⊥ Y. Nishimura,⊥ and S. Ishii‡

Life Science Center, The Institute of Chemical & Physical Research (RIKEN), 3-1-1 Koyadai, Tsukuba, Ibaraki, 305 Japan, National Institute of Bioscience and Human-Technology, 1-1 Higashi, Tsukuba, Ibaraki, 305 Japan, Institute of Basic Medical Science, University of Tsukuba, Tsukuba, Japan, and Graduate School of Integrated Science, Yokohama City University, Seto, Kanazawa-ku, Yokohama, 236 Japan

Received March 1, 1993

ABSTRACT: The DNA-binding domain of the *c-myb* protooncogene product consists of three homologous tandem repeats of 51–52 amino acids (denoted as R1, R2, and R3 from the N-terminal side). In order to analyze conformational and thermodynamic characteristics of the homologous repeats, we have examined the DNA-binding domain by circular dichroism (CD) and differential scanning calorimetry (DSC). The CD spectra for the three individual repeats are significantly different in the fine profiles, indicating subtle differences in their conformations. The melting analyses for the fragments show that the thermal stability of each fragment is different from one another, with the following order of stability: R1(T_m = 61 °C) ≳ R3(57 °C) ≫ R2(43 °C), where R2 is much less stable than the other repeats. The denaturing process for the whole DNA-binding domain, measured by DSC, is characterized by a very broad transition ranging from 30 to 80 °C. The denaturation curve can be fit well by a three-state transition with one intermediate state. The transition temperature for the native-to-intermediate transition coincides with the melting temperature of R2, indicating that the intermediate state corresponds to the unfolding of unstable R2. The CD spectrum of the whole domain is almost identical to the sum of the individual spectra. Thus, these results suggest that the individual repeats in the whole DNA-binding domain behave independently in terms of conformation and stability. The addition of DNA to the DNA-binding fragment drastically changed the melting profile, in which the broad transition curve was replaced by a sharp peak at 58 °C. The stability of the binding domain is apparently increased by DNA, and the transition becomes cooperative. On the other hand, simultaneous measurements by CD have indicated that the secondary structure of the domain is not changed by the presence of DNA. We discuss the implications of these results on the role of each repeat in the DNA binding and sequence recognition by Myb.

The protooncogene *c-myb* codes for the nuclear protein which binds to DNA in a sequence-specific manner (Biedenkapp *et al.*, 1988; Nakagoshi *et al.*, 1990). The c-Myb protein can function as an activator or repressor of transcription (Nishina *et al.*, 1989; Weston & Bishop, 1989; Nakagoshi *et al.*, 1989; Ness *et al.*, 1989). The DNA-binding domain of c-Myb consists of three homologous tandem repeats of 51–52 amino acids (Gonda *et al.*, 1985; Klempnauer & Sippel, 1987; Sakura *et al.*, 1989). Each repeat has three conserved tryptophans spaced 18–19 amino acids apart. The solution structure of the third repeat (R3) has been determined by NMR analysis (Ogata *et al.*, 1992). The analysis showed that the conserved tryptophans form a hydrophobic core, as predicted from sequence and mutagenesis analyses (Kanei-Ishii *et al.*, 1990; Saikumar *et al.*, 1990), and that α-helices fold into a conformation similar to a helix–turn–helix (HTH) motif. R3 is supposed to recognize the core AAC sequence in the consensus Myb binding sites, 5′-(C/Pu)(Py/A)-PyAACPyPu-3′, with one of the helices interacting directly with base pairs. On the other hand, the role of the first and second repeats in DNA binding is unknown. The first repeat (R1) can be deleted without significant loss of DNA-binding activity (Sakura *et al.*, 1989; Howe *et al.*, 1990). The second repeat (R2) has been suggested to take on an HTH-related motif on the basis of the experimental result that mutations of corresponding amino acids in R2 and R3 affected specific DNA-binding activity in the same way (Gabrielsen *et al.*, 1991). However, this has not yet been proven by structural analyses.

When the sequences of the three repeats are aligned, those amino acids which are found to form a hydrophobic core in R3 are not perfectly conserved in R1 and R2. Thus, each repeat may take a different conformation or exhibit different intrinsic stability. Such different characteristics may be related to the functional role of each repeat in the specific recognition of DNA. In order to analyze conformational and thermodynamic characteristics of the homologous repeats, we have examined the DNA-binding domain of Myb by circular dichroism (CD) and differential scanning calorimetry (DSC).

MATERIALS AND METHODS

The fragment containing three repeats (R123) was prepared as follows. Bacteria BL21(DE3) carrying pAR2156*myb*R123 were grown, and the expression of the c-Myb R123 was induced by the addition of isopropyl β-D-thiogalactopyranoside. R123 was recovered in the soluble fraction of the bacterial extract and purified by DEAE–cellulose and phosphocellulose column chromatography. R123 was eluted from the DEAE–cellulose column with 0.4 M NaCl and from the phosphate column with 0.6 M NaCl. The purity of R123 was determined to be about 95% by SDS–polyacrylamide gel electrophoresis as described (Kanei-Ishii *et al.*, 1990). The purified R123 was dialyzed against 50 mM potassium phosphate buffer (pH 7.5)

† This work was partly supported by special-grants-in-aid (02263104) from the Ministry of Education, Science and Culture of Japan.

* Author to whom correspondence should be addressed.
‡ The Institute of Chemical & Physical Research.
§ National Institute of Bioscience and Human-Technology.
∥ University of Tsukuba.
⊥ Yokohama City University.

0006-2960/93/0432-7759$04.00/0

containing 50 mM KCl. The synthetic R1, R2, and R3 fragments are kind gifts from Dr. Aimoto (Hojo & Aimoto, 1991).

The 22-mer oligo-DNA, d(CACCCTAACTGACACA-CATTCT), which contains the Myb binding site in SV40 enhancer, MBS-I, and its complementary strand were synthesized and purified by HPLC with a C18 reverse-phase column (WAKO-SIL DNA). The oligo-DNA was suspended in 1 × STE and annealed with a complementary strand to yield double-stranded DNA. The purified DNA was dialyzed against the same buffer as in Myb simultaneously.

Calorimetric measurements were carried out on an MC-2 (Microcal) differential scanning calorimeter. Data were collected in the temperature range between 5 and 100 °C at a heating rate of 0.75 °C/min, unless indicated otherwise. Protein and DNA concentrations were 2.2 and 1.6 mg/mL, respectively, to give an equimolar partition, unless indicated otherwise. Heat capacity functions were analyzed by the double deconvolution procedure (Kidokoro & Wada, 1987). The initial parameter set obtained by the procedure was further adjusted by a nonlinear least-squares fitting method (Kidokoro *et al.*, 1988), using the SALS program (Nagasawa & Oyanagi, 1980).

CD spectra in the range 190–290 nm were recorded on a Jasco J600 spectropolarimeter using standard procedures. Measurements were made using a cylindrical fused quartz cell with a 0.02-cm path length. Melting curves were recorded at 222 and 274 nm using the same cell with a circulating water bath surrounding the cell. Data were collected in the temperature range between 10 and 85 °C at a heating rate of 0.75 °C/min.

RESULTS

Reversibility of Myb Denaturation. We first checked the reversibility of the denaturation process of Myb DNA-binding domains. Thermal melting of R1 and R123 was measured by CD at different heating rates, 0.75 and 0.5 °C/min. The melting curves were identical for the different heating rates. Thus, we used 0.75 °C/min for the rest of the measurements.

We also checked whether the denaturation process depends on the sample concentration. We measured the melting of R123 by CD at two different sample concentrations, 2.2 and 1.1 mg/mL. The melting curves were identical for the different concentrations. Thus, the denaturation process does not seem to involve concentration-dependent phenomena such as protein–protein interaction and aggregation of unfolded proteins.

Conformation and Stability of Homologous Repeats: R1, R2, and R3. Figure 1 shows the CD spectra of R1, R2, and R3 fragments. As one can see from the spectra, they show typical α-helical characteristics. The α-helix content of these fragments estimated by the method of Chen *et al.* (1974) is 50–60%. On the other hand, individual spectral curves are significantly different from one another in the wavelength range between 210 and 230 nm. This difference in the CD spectra indicates that there will be subtle differences in the conformations of the repeat fragments.

Figure 2 shows the thermal denaturation of R1, R2, and R3 fragments measured by CD. It is apparent from this result that R2 is much less stable than the others, characterized by a broad transition curve. The differentiation of the melting curve shows that T_m as defined by a peak is about 43 °C. The denaturation curves of R1 and R3 are similar, in which both start melting near 40 °C. The derivatives of the transition curves indicate that R1 is slightly more stable than R3, with their T_m values being 61 and 57 °C, respectively. Thus, the order of thermal stability of the three repeats in the Myb DNA binding is R1 ≳ R3 ≫ R2.

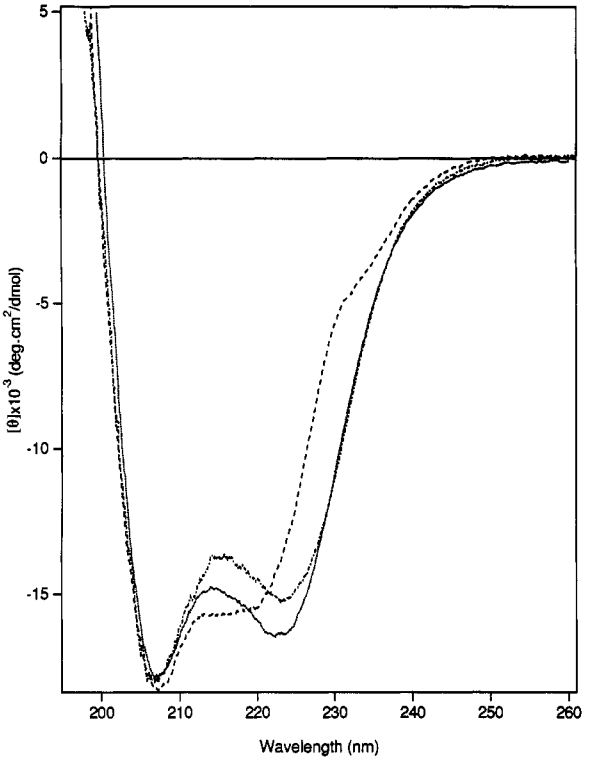

FIGURE 1: CD spectra of R1 (···), R2 (– · –) and R3 (– –) fragments. Protein concentration is 2.2 mg/mL in 50 mM potassium phosphate buffer (pH 7.5) with 50 mM KCl. The vertical scale is normalized by the mole concentrations.

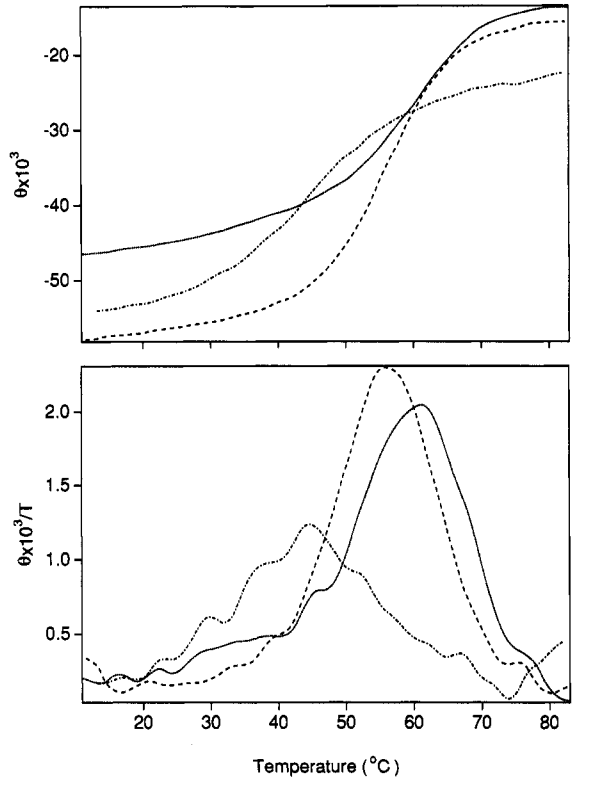

FIGURE 2: (a, Top) Melting curves of R1 (···), R2 (– · –), and R3 (– –) monitored at 222 nm. The derivatives for the corresponding curves are shown in b (bottom). The curves were smoothed by averaging over 15 points in a 0.93 °C window.

Denaturation of the Whole DNA-Binding Domain of Myb. Figure 3 shows the DSC curve of the R123 fragment. It is

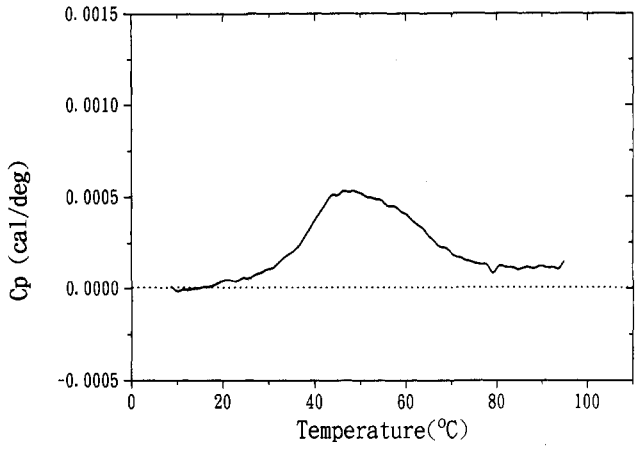

FIGURE 3: DSC curve of the Myb R123 fragment. Protein concentration is 2.2 mg/mL in 50 mM potassium phosphate buffer (pH 7.5) with 50 mM KCl.

characterized by a very broad transition, which starts around 30 °C and ends around 80 °C. It is also characterized by an asymmetric shape with a shoulder at the high-temperature side. A very similar transition was obtained by the CD melting. Thus, the conformational change monitored by CD is in parallel with the thermal denaturation process monitored by DSC. From these results, it is apparent that the transition cannot be fit by a simple two-state model with native and denatured states. In fact, the ratio of calorimetric enthalpy, ΔH^{cal}, and van't Hoff enthalpy, ΔH^{vH}, at denaturation mid-temperature (49.8 °C), estimated from the DSC curve, is $\Delta H^{cal}/\Delta H^{vH} = 3.1$, indicating the presence of intermediate states.

We have analyzed the transition by three-state and four-state models. The fit by the three-state model is quite good, as shown in Figure 4a. The four-state model slightly improved the fitting in the low-temperature tail region. The RMSD between the calculated and measured heat capacity curves for the two-state model is 66.7 μcal/K, whereas those for the three-state and four-state models are 6.7 and 4.5 μcal/K, respectively. Since the precision or reproducibility of this instrument is on the order of 25 μcal/K, we cannot distinguish between the three-state model and the four-state model within the instrumental precision. Figure 4b shows the calculated mole fractions of each state from the heat capacity curve based on the three-state model. One can see that the native state is transformed to the denatured state via an intermediate state. The transition temperature, T_{01}, for the native-to-intermediate transition, defined by the crossing point between the native and intermediate mole fraction curves (f_N and f_I), is 42.7 °C from Figure 4b, whereas the native-to-denatured transition temperature, T_{02}, is 51.2 °C. The intermediate-to-denatured transition temperature, T_{12}, which is defined by the crossing point between f_I and f_D, is 61 °C. T_{01} coincides with the T_m of R2, whereas T_{12} coincides with the T_m of R1 (also close to that of R3). These results indicate that the intermediate state corresponds to the unfolding of R2, and its decay represents the denaturation of R3 and R1. Thus, this result also suggests that the three repeats in R123 behave as independent units in terms of stability.

Effect of DNA on the Conformation and Stability of the Myb DNA-Binding Domain. Figure 5 shows the CD spectrum of the Myb R123 fragment. The conditions of the sample are the same as those in the DSC measurements. Compared with the spectra of R1, R2, and R3 (Figure 1), the spectrum of R123 is very close to the average of the three spectra. This suggests that the structures of R1, R2, and R3 remain intact

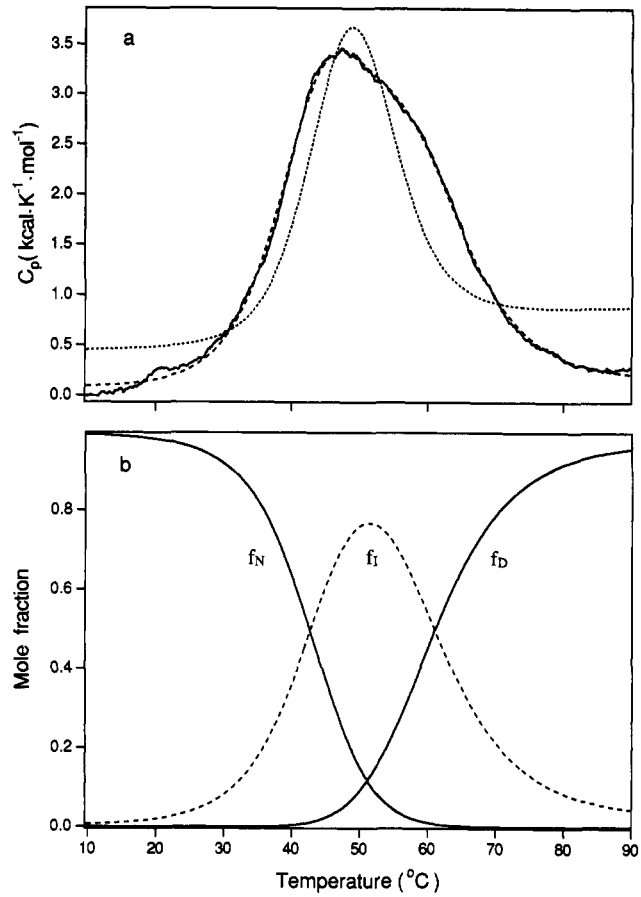

FIGURE 4: (a) Experimental (—) and calculated (– –) heat capacity curves of the Myb R123 fragment. The calculated curve is based on the three-state model with one intermediate state. For the sake of comparison, fitting by the two-state model is also shown (- - -). (b) Mole fractions of native (f_N), intermediate (f_I), and denatured (f_D) states for the Myb R123 fragment, estimated by the three-state model.

in the R123 fragment. Also shown in Figure 5 is a CD spectrum of R123 in the presence of the MBS-I DNA fragment. This spectrum was derived by subtracting the spectrum of DNA alone (not shown) from the spectrum of a mixture of R123 and DNA. One can see that this spectrum is very similar to that for the protein alone. Thus, this result indicates that the secondary structure of the Myb R123 fragment is not changed significantly by the presence of DNA.

Figure 6 shows the DSC curve of the 22-mer MBS-I DNA fragment. It is characterized by a very sharp transition, with a peak at 68 °C, and a small tail at the low-temperature side. This transition corresponds to the thermal melting of a double strand to single strands and, thus, represents a typical dimer–monomer transition. The curve can be fit by a simple two-state model with marginal differences in the low-temperature tail, which may be due to the premelting of the terminal region. The thermally induced melting of the MBS-I DNA fragment monitored by CD at 274 nm yielded a transition curve similar to the one obtained by the DSC measurement.

Equimolar DNA and protein were mixed so as to yield the same DNA and protein concentrations as in Figures 4 and 6, and the mixture was analyzed by DSC. As shown in Figure 7, the denaturation of R123 shows a very different melting profile in the presence of DNA. The broad transition of Myb disappears, and instead a very sharp transition with a peak near 58 °C appears. A peak corresponding to DNA melting remains at the same position. Consequently, for the first approximation, the thermal transition of the R123–DNA complex involves stepwise transitions of DNA-bound R123

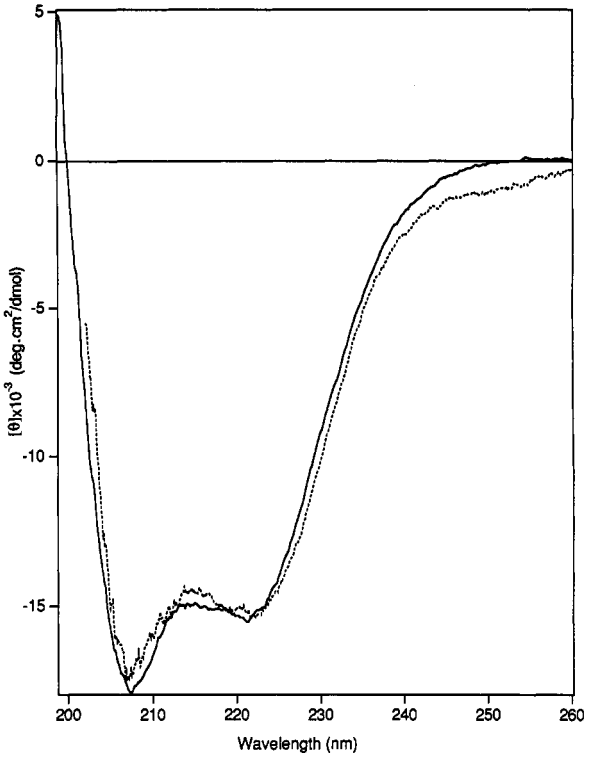

FIGURE 5: CD spectra of free Myb R123 (—) and R123 in the presence of MBS-I DNA (- - -). The conditions of the sample are the same as those in the DSC measurements. The spectrum of R123 in the presence of DNA was obtained by subtracting the spectrum of MBS-I from that of the mixture of R123 and MBS-I. The vertical scale is normalized by the mole concentrations.

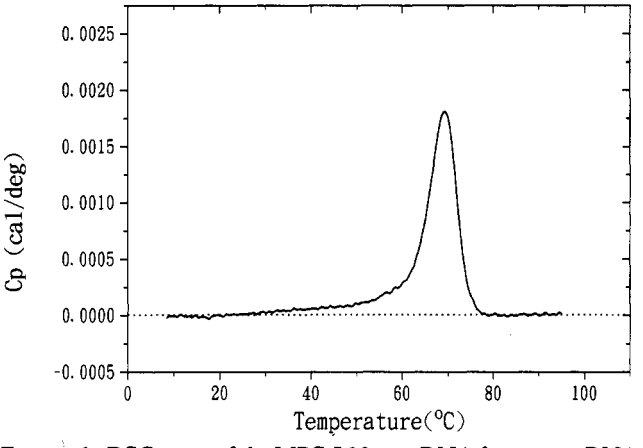

FIGURE 6: DSC curve of the MBS-I 22-mer DNA fragment. DNA concentration is 1.6 mg/mL. Other conditions are the same as in Figure 1.

and DNA. Because the shape and location of melting curve of DNA in the Myb–DNA complex are similar to those of free DNA, we subtract the DNA denaturation curve (Figure 6) from the present melting profile to obtain the denaturation curve of Myb in the presence of DNA. This results in a single-peak transition curve. We obtained a similar transition curve by CD melting analysis for the Myb–DNA complex. As the curve was analyzed by a two-state model, the low-temperature tail was not fit well (RMSD is 55 μcal/K). Analysis by the three-state model suggests that there is a minor intermediate state which decays along with the native state. The RMSD for the three-state model (on the order of 30 μcal/K) is still larger than the instrumental precision (25 μcal/K). This is probably due to the simplified procedure for the estimation of Myb denaturation in the presence of DNA, in which the

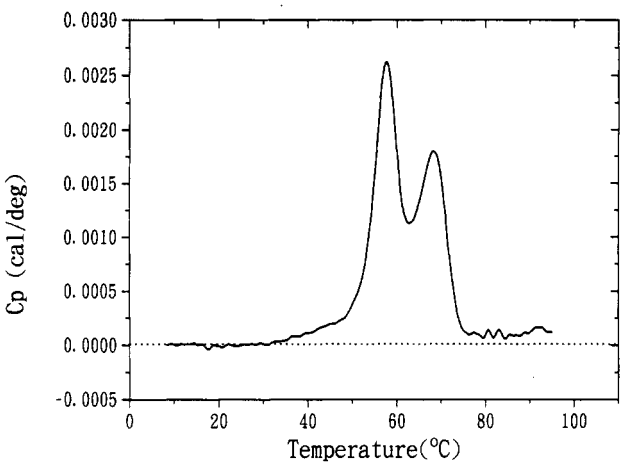

FIGURE 7: DSC curve of the mixture of R123 and MBS-I DNA. Protein and DNA concentrations are the same as in Figures 3 and 6.

Table I: Thermodynamic Characteristics for the Thermal Transition of the Myb DNA-Binding Domain and the MBS-I DNA Fragment[a]

	DNA (free)[b]	Myb (free)	Myb (complex)[c]
Native-to-Intermediate Transition			
T_{01} (°C)[d]	67.8 ± 0.03[e]	42.7 ± 0.3	52.5 ± 0.9
ΔH_{01} (kcal/mol)	141.4 ± 0.5	41.9 ± 0.8	29.4 ± 1.0
ΔC_{01} (kcal K^{-1} mol^{-1})	0	0.84 ± 0.1	−1.0 ± 0.2
Native-to-Denatured Transition			
T_{02} (°C)		51.2 ± 0.1	55.7 ● 0.1
ΔH_{02} (kcal/mol)		94.0 ± 1.1	132.1 ± 1.4
ΔC_{02} (kcal K^{-1} mol^{-1})		0.05 ± 0.01	1.03 ± 0.36

[a] Calculations for free Myb and complexed Myb were based on the three-state model, and enthalpies and heat capacities relative to the native state are shown. [b] The heat capacity curve of MBS-I DNA in the Myb–DNA complex is nearly identical to that of free DNA. [c] The thermodynamic quantities were estimated for the transition curve in which the DNA denaturation curve (Figure 6) is subtracted from that of the Myb–DNA complex (Figure 7). [d] The transition temperatures, T_{01} and T_{02}, are defined as the temperatures where the mole fraction of the native state crosses with those of the intermediate state and the denatured state, respectively (see Figure 4b). [e] The values in this table were calculated by the least-squares fitting procedure described in the text. The error values represent the fitting error calculated by an error matrix during the fitting, and they do not contain the error due to sample concentrations.

DSC curve of DNA is subtracted from that of the Myb–DNA complex.

Table I summarizes the thermodynamic quantities derived from the DSC analyses for DNA, Myb, and Myb bound to DNA. The thermodynamic quantities for Myb and Myb bound to DNA were calculated on the basis of the three-state model. The transition enthalpy and heat capacity change were estimated by the method described in the previous section. The larger enthalpy change for the denaturation of Myb in the presence of DNA will include the contribution from the interaction between Myb and DNA.

DISCUSSION

The CD spectra of R1, R2, and R3 have indicated that these repeats have subtle differences in their conformations. Preliminary NMR analyses (K. Ogata *et al.*, unpublished results) have indicated that the conformations of R1 and R2 may be different from that of R3. The stability analyses of the three individual repeats showed the differences in their stabilities as well, with the following stability order: R1 ≳ R3 ≫ R2, where R2 is much less stable than R1 and R3.

Figure 8 shows the alignment of the amino acid sequences of R1, R2, and R3. Although the three tryptophans are

```
R1  LGKTRWTREE DEKLKKLVEQ NGTDDWKVIA NYLPNRTDVQ CQHRWQKVLN PE
    38         48         58         68         78         88
R2  LIKGPWTKEE DQRVIKLVQK YGPKRWSVIA KHLKGRIGKQ CRERWHNHLN PE
    90         100        110        120        130        140
R3  VKKTSWTEEE DRIIYQAHKR LG.NRWAEIA KLLPGRTDNA IKNHWNSTMR RK
    142        152        162        171        181        191
```

FIGURE 8: Alignment of amino acid sequences of R1, R2, and R3. Aliphatic hydrophobic amino acids are marked by shaded boxes, and aromatic amino acids are indicated by open boxes. The locations of α-helices in R3 are underlined.

conserved, other hydrophobic and aromatic amino acids, which play an important role in forming the hydrophobic core, are not perfectly conserved. According to the NMR structure of R3 (Ogata *et al.*, 1992), three α-helices, underlined in Figure 8, are maintained by a hydrophobic core formed by Trp 147, Ile 154, Ile 155, His 159, Trp 166, Ile 169, Leu 173, Ile 181, His 184, Trp 185, and Met 189. Some of these amino acids are not conserved in R1 and R2. The NMR structure of R3 shows that Trp 147 interacts with His 184 and that Trp 185 and Trp 166 interact with His 159. In general, interactions of aromatic side chains are thought to contribute to the stability of the hydrophobic core of proteins (Blundell *et al.*, 1986). R2 does not have histidines at these positions, whereas R1 has His 80 adjacent to the latter position. Although we cannot quantitatively correlate the structure and stability of proteins with amino acid sequences, those sequence differences in the hydrophobic core region may be responsible for the experimentally observed differences in the conformation and stability of the homologous repeats.

The DSC measurement of R123 has indicated that the denaturation of R123 involves an intermediate state. This is consistent with the stability analysis of the individual repeats, which indicated unstable R2 and stable R3 and R1. The intermediate state in the denaturation of R123 can be explained by the unfolding of R2. Indeed, the transition temperature, T_{01}, of R123 (42.7 °C, see Table I) agrees with the T_m (43 °C) defined by the peak of the derivative of the R2 melting curve. The melting of R1 and R3 would correspond to the decay of the intermediate state, and the transition temperature, T_{12}, for the intermediate-to-denatured transition of R123 coincides with the T_m of R1. As mentioned previously, the stability of R3 may be too close to that of R1 for their differential melting to be resolved within instrumental precision. Thus, the stability analyses of the R123 fragment, together with the analyses of the individual repeats, suggest that each repeat in R123 behaves as an independent unit in the denaturation process, and the denaturation proceeds with successive melting of each repeat. On the other hand, the CD spectrum of R123 is almost identical to the averaged CD spectrum from the three individual spectra, suggesting that each repeat in the DNA-binding domain of Myb can be considered independent in terms of its conformation as well.

The conformation and stability of DNA-binding proteins can be affected by the binding to their target DNA sequences. It has been indicated that binding of homodimers of *c-jun* protooncogene products, Jun, or heterodimers of Jun and *c-fos* protooncogene products, Fos, which are known to associate through leucine zipper structures, to a specific DNA target sequence, the AP-1 site, causes a change in conformation that results in increased α-helicity (Patel *et al.*, 1990). Also, another yeast transcription factor, GCN4, increases the α-helix content of its DNA-binding domain from 70% to at least 95% in the presence of DNA containing a GCN4 binding site, the AP-1 site (Weiss *et al.*, 1990). These results indicate that the α-helix structures of the proteins are stabilized as these proteins form a complex with DNA. Therefore, we have examined whether the conformation of the Myb DNA-binding domain is affected by the presence of its target DNA. However, the CD spectra of free R123 and R123 in the presence of the MBS-1 DNA fragment show that the secondary structure of the R123 fragment is not significantly affected by the presence of DNA. This is true for room temperature. At higher temperatures, where free Myb is partly denatured, the addition of DNA would stabilize the protein structure, increasing its α-helix content. The α-helix content of R123 at room temperature is estimated to be about 56%, which roughly agrees with the 60% α-helix of R3 derived from the NMR structure. The present result indicates that this secondary structure of the Myb DNA-binding domain is not significantly changed by the specific binding to DNA.

On the other hand, addition of DNA to R123 drastically increases the stability of R123. Also, the transition of R123 becomes much sharper in the presence of DNA than that of free R123. DSC and CD measurements gave similar results with respect to this conclusion. The comparison of the transition curve of R123 in the presence of DNA with those of the R1, R2, and R3 fragments obtained by CD analyses show that the melting temperature of R123 in the presence of DNA becomes close to those of the R3 and R1 fragments. Thus, R2, when bound to DNA, apparently behaves like the other repeats in terms of stability, and all of the repeats seem to denature in a cooperative manner.

The DNA-binding domain of Myb has a unique structure, in which three homologous units are repeated in tandem. The role of R1 is unclear but it may not play critical role in the recognition of DNA sequence, since it can be deleted without serious loss of specific DNA-binding activity of Myb (Sakura *et al.*, 1989; Howe *et al.*, 1990). However, the fact that R1 is the most stable repeat suggests that R1 can play some structural role in the nonspecific binding of Myb to DNA. The HTH-related structure of R3 is thought to play an important role in recognizing the core AAC sequence in the consensus Myb binding site. This unit was shown to have a stable structure. R2 has been proposed to have an HTH-like structure and play the same role as R3 (Gabrielsen *et al.*, 1991). However, the present analyses have shown that R2 has a conformation significantly different from that of R3 and is much less stable and more flexible than R3. These distinctive characteristics of R2 rather suggest that R2 will play different role in the recognition of DNA. It is interesting that the least stable unit is sandwiched by the stable units. This may have some relevance to the DNA-binding mode of Myb. The present analyses of the Myb DNA-binding domain by DSC and CD measurements indicate that the conformation and stability may correlate with the functional roles of each repeat in the Myb DNA-binding domain.

ACKNOWLEDGMENT

We thank Dr. Saburo Aimoto for providing us with the synthetic fragments of Myb DNA-binding domains and Mr. Y.-F. Wang for helping with the manuscript preparation.

REFERENCES

Biedenkapp, H., Borgmeyer, U., Sippel, A. E., & Klempnauer, K.-H. (1988) *Nature 335*, 835–837.

Blundell, T., Singh, J., Thornton, J., Burley, S., & Petsko, G. (1986) *Science 234*, 1005.

Chen, Y.-H., Yang, J. T., & Chau, K. H. (1974) *Biochemistry 13*, 3350–3359.

Gabrielsen, O. S., Sentenac, A., & Fromageot, P. (1991) *Science 253*, 1140–1143.

Gonda, T. J., Gough, N. M., Dunn, A. R., & de Blaquiere, J. (1985) *EMBO J. 4*, 2003–2008.

Hojo, H., & Aimoto, S. (1991) *Bull. Chem. Soc. Jpn. 64*, 111–117.

Howe, K. M., Reaks, C. F. L., & Watson, R. J. (1990) *EMBO J. 9*, 161–169.

Kanei-Ishii, C., Sarai, A., Sawazaki, T., Nakagoshi, H., He, D.-M., Ogata, K., Nishimura, Y., & Ishii, S. (1990) *J. Biol. Chem. 265*, 19990–19995.

Kidokoro, S., & Wada, A. (1987) *Biopolymers 26*, 213–229.

Kidokoro, S., Uedaira, H., & Wada, A. (1988) *Biopolymers 27*, 271–279.

Klempnauer, K.-H., & Sippel, A. E. (1987) *EMBO J. 6*, 2719–2725.

Nagasawa, T., & Oyanagi, Y. (1980) in *Recent Development in Statistical Inference and Data Analysis* (Matsushita, K., Ed.) pp 221–225, North Holland Publishing Co., Amsterdam.

Nakagoshi, H., Nagase, T., Ueno, Y., & Ishii, S. (1989) *Nucleic Acids Res. 17*, 7315–7324.

Nakagoshi, H., Nagase, T., Kanei-Ishii, C., Ueno, Y., & Ishii, S. (1990) *J. Biol. Chem. 265*, 3479–3483.

Ness, S. A., Marknell, A., & Graf, T. (1989) *Cell 59*, 1115–1125.

Nishina, Y., Nakagoshi, H., Imamoto, F., Gonda, T. J., & Ishii, S. (1989) *Nucleic Acids Res. 17*, 107–117.

Ogata, K., Hojo, H., Aimoto, S., Nakai, T., Nakamura, H., Sarai, A., Ishii, S., & Nishimura, Y. (1992) *Proc. Natl. Acad. Sci. U.S.A. 89*, 6428–6432.

Patel, L., Abate, C., & Curran, T. (1990) *Nature 347*, 572–575.

Saikumar, P., Murali, R., & Reddy, E. P. (1990) *Proc. Natl. Acad. Sci. U.S.A. 87*, 8452–8456.

Sakura, H., Kanei-Ishii, C., Nagase, T., Nakagoshi, H., Gonda, T. J., & Ishii, S. (1989) *Proc. Natl. Acad. Sci. U.S.A. 86*, 5758–5762.

Weiss, M. A., Ellenberger, T., Wobbe, C. R., Lee, J. P., Harrison, S. C., & Struhl, K. (1990) *Nature 347*, 575–578.

Weston, K., & Bishop, J. M. (1989) *Cell 58*, 85–93.